J Mater Sci (2011) 46:5017–5028
DOI 10.1007/s10853-011-5422-y

Medium-density ablative composites: processing, characterisation and thermal response under moderate atmospheric re-entry heating conditions

Bibin John · Dona Mathew · B. Deependran · George Joseph · C. P. Reghunadhan Nair · K. N. Ninan

Received: 5 December 2010 / Accepted: 26 February 2011 / Published online: 15 March 2011

Abstract Medium-density foam composites based on silica fibre-filled phenolic syntactic foams were processed and characterised for mechanical, dynamic mechanical and thermophysical properties, and they were evaluated as Thermal Protection Systems (TPSs) materials by way of experiment and simulated thermal response studies under atmospheric re-entry conditions. Ablative composites with different specific gravities were processed by varying the volume fraction of the constituents. Tensile strength increased with fibre concentration and showed a maximum corresponding to 15% by volume of silica fibre and decreased on further addition, whereas flexural and compressive strength increased with increase in volume percentage of silica fibre. The mechanical properties of the fibre reinforced system were superior compared to those of bare phenolic syntactic foams. Storage modulus was considerably improved by the addition of fibre whilst the glass transition temperature was unaffected. The compositional dependency of the ablative composites on their thermophysical properties and thermal degradation behaviour was also examined. The thermal response of the ablatives was studied by simulating a moderate atmospheric re-entry heat flux history on the specimen with a maximum heat flux of about 15–18% of the stagnation heating. The thermal response was measured, and the material surface behaviour, mass loss and flammability were studied. For fibre fractions corresponding to various specific gravities, the thermal simulation experiments were studied, and it was observed that the char strength and its structural integrity were satisfactory for a specific gravity of 0.5. The maximum backwall temperature measured was 110 °C for a test duration of 500 s, and this meets the structural temperature constraint of 150 °C at the interface. The thermal response was numerically modelled, and fairly good comparison was obtained with the experimental results. This validated the accuracy of the measurement of the thermophysical properties and delivered the medium-density ablative TPS system qualified for application in atmospheric re-entry.

B. John
Lithium Ion and Fuel Cell Division, Vikram Sarabhai Space Centre, Thiruvananthapuram 695 022, India
e-mail: bbnjohn@yahoo.com

D. Mathew · C. P. Reghunadhan Nair (✉)
Polymers and Special Chemicals Division, Vikram Sarabhai Space Centre, Thiruvananthapuram 695 022, India
e-mail: cprnair@gmail.com

D. Mathew
e-mail: dona_mathew@vssc.gov.in

B. Deependran · G. Joseph
Aerodynamic Heating and Thermal Analysis Division, Vikram Sarabhai Space Centre, Thiruvananthapuram 695 022, India
e-mail: b_deependran@vssc.gov.in

K. N. Ninan
Department of Chemistry, Indian Institute of Space Science and Technology, Thiruvananthapuram 695 547, India

Introduction

During atmospheric re-entry, space vehicles are subjected to severe aerodynamic heating, and their successful return through the earth's atmosphere largely depends on the provision made for reducing aerodynamic heat transfer to the structure. The high heat flux condition as encountered during atmospheric re-entry warrants efficient thermal protection systems (TPSs). Ablatives form a class of TPS, which undergoes physical, chemical and mostly endothermal transformations. These transformations produce new liquid or gas phases, which are subsequently injected into

the environment [1]. When mass is a constraint, the preference is for low mass fraction TPS like low-density ablatives which function against moderate aero-thermal environments during atmospheric re-entry whilst maintaining the TPS weight penalty at the minimum. They can occupy fairly large areas of the re-entry capsule at regions away from the stagnation zone. Functionality of these materials can be tailored to meet the requirements for a given location depending on the extent of aero-heating, without changing the TPS material from region to region.

Thermal protection systems in the form of low-density syntactic foams (microsphere filled polymers) are advantageous in reducing the lift-off weight of the launch vehicle. Further, they are found to be strong enough to encounter the aerodynamic shear. Epoxy, phenolic and silicone-based syntactic foams have been successfully used for thermal protection of atmospheric re-entry space vehicles and to prevent structures from the extreme heat flux of rocket exhaust plumes [2–9]. The latent heat of evaporation of the resin allows extremely high temperatures to be withstood for short periods as in the case of rockets and other re-entry space vehicle systems [6]. Syntactic foams provide the flexibility of modifying the physical and mechanical properties as per requirement, by varying the composition of constituents [2]. Also, in a given composition of resin and filler, it is further possible to tailor the mechanical properties and density by varying the nature/composition/s of the fillers and the extent of compaction. Thus, density can be maintained a minimum by limiting the extent of mechanical compaction (for achieving the minimum required structural strength). This leaves high porosity in the system, resulting in low thermal conductivity, rendering them suitable for use as passive thermal insulation materials as well as ablative systems.

The thermal degradation of ablators based only on polymers usually produces weak and brittle char, which is susceptible to rapid removal by the mechanical forces produced as an effect of the elevated re-entry speeds, which results in reduction of the thermal insulation. One of the roles of the char is to limit oxygen diffusion from the boundary layer to the bulk to prevent the exothermic degradation reactions of the polymeric matrix. Therefore, the mechanical characteristics and the physio-chemical properties of the char are of fundamental importance to ensure good quality of an ablative material. Reinforcing fibres and other inorganic fillers must be therefore included in the ablative formulation to improve the char stability [9]. Also, the incorporation of fibrous reinforcements is a known method for strengthening syntactic foams [10–13]. In view of this, silica fibre reinforced, phenolic syntactic foams are considered as appropriate candidates for atmospheric re-entry TPS applications.

This article describes the processing of silica fibre-reinforced phenolic syntactic foams containing varying concentration of silica fibre and different specific gravities. The compositional dependency of the mechanical, dynamic mechanical, thermal and thermophysical properties of the foam composites was also examined. The properties of the fibre reinforced systems are compared with those of bare phenolic syntactic foams. Thermal response of the ablatives was studied by simulating a moderate atmospheric re-entry heat flux history on the specimen with maximum heat flux of about 40 W/cm^2 for duration of 600 s. Material surface behaviour, mass loss and flammability were studied and correlated to the functional requirements of a typical flight.

Experimental

Materials

The phenolic resin (resole type) used for processing the ablative composites was synthesized by the reaction of phenol and formaldehyde in the presence of triethyl amine as catalyst by a proprietary process developed in VSSC. The resin has a solid content of 72.5% and possesses 16% free phenol. The density of the cured resin system is 1200 kg/m^3. Glass microballoons K-37 and K-25, supplied by 3M Company, USA, were used as low-density fillers. The properties of the microballoons are given in Table 1. Silica fibres (silica content >99%) in the form of chopped strands of length 4–7 mm provided by M/s. Valeth High Tech composites, Chennai, India, were used as such without any sizing agent.

Processing of the syntactic foams

Weighed amount of phenolic resin was mixed with silica fibre in a beaker till all the fibre was wet with phenolic resin. Required quantity of microballoon was then added

Table 1 The properties of K-25 and K-37 glass microballoons as provided by the manufacturer

Microballoon type	Microballoon size distribution (μm, by volume at different percentiles)			Effective top size (μm)	Target fractional survival (%)	Average true particle density (kg/m^3)	Thermal conductivity (W/mK) at 70°F (21 °C)
	10th	50th	90th				
K-25	25	55	90	105	90	250	0.085
K-37	20	45	80	85	90	370	0.124

and thoroughly mixed to get a uniform dispersion of microballoon. Mixing was done gently to avoid breaking of microballoons. This particular route of addition of fibre followed by addition of microballoon has been reported to lead to better mechanical performance for fibre-reinforced syntactic foams [10]. The mixture was then placed in a rectangular mould and compression moulded to the required thickness. For processing bare phenolic syntactic foams, phenolic resin was mixed with microballoon and then compression moulded. The moulding pressure was ~5 MPa. The curing was done according to the schedule 100 °C (1/2 h), 125 °C (1/2 h), 150 °C (1 h) and 180 °C (2 h). The composition and density of the syntactic foams were determined. Phenolic syntactic foams without fibre are designated as PS and those with fibre as PSF.

Silica fibre-reinforced phenolic syntactic foams with varying fibre loadings were processed. The formulations used for processing the composites were phenolic resin: microballoon: silica fibre = 100:80: (0, 30, 50, 70, 90 and 100) (by weight). The composition and density of the processed composites are given in Table 2. From the table, it is clear that, the density of the composites increased with increase in concentration of fibre.

The density and properties of syntactic foams can further be tuned for a given composition using microballoons with low density and shell thickness. Thus, a composition of PSF1, denoted as PSF1-M, containing two types of microballoons; K25 and K37 in equal weight ratios resulted in syntactic foam with a density of 500 kg/m^3 and total porosity of 8.5%. During the processing of syntactic foams, entrapment of air may occur leading to voids, which would affect the properties of the composite. The void percentage has been calculated using the relation

$$\text{Void percentage} = \frac{V - V_f - [(W - W_f) \times W_R/\rho_R + (W - W_f) \times W_M/\rho_M]}{V} \times 100$$

where V and W are the volume and weight of foam block; V_f and W_f are the volume and weight of fibre; W_R and W_M are the weight fractions of resin and microballoon; ρ_R and ρ_M are the densities of resin and microballoon, respectively.

Characterization of the ablative composites

Test specimens with dimensions conforming to ASTM D-3039, ASTM D-790 and ASTM D-695 were used for evaluating tensile, flexural and compressive properties, respectively. The specimen dimension was 5 × 13 × 69, 5 × 13 × 100 and 5 × 5 × 10 mm, respectively, for tensile, flexural and compressive strength determination. The testing was done in Universal Testing Machine Instron Model 4202. The three point bending test was conducted for flexural strength measurement at a cross head speed of 2.1 mm/min. Tensile and compressive strength testing were conducted at a cross head speed of 5 mm/min. The configuration of the specimen used for tensile measurement was dogbone with wide ends and a narrow middle, conforming to ASTM D-3039. All the measurements were carried out at room temperature. The fracture surface morphology of the ablative composites was studied by Scanning Electron Microscopy. The samples were sputtered with a conducting layer of gold and examined in a Philips XL-30 Scanning Electron Microscope.

Dynamic mechanical measurements were conducted on Rheometrics Scientific model Mark IV (UK) at a frequency of 1.0 Hz and a heating rate of 10 °C/min in the bending mode. The sample dimension was 4 × 10 × 28 mm^3.

Coefficient of thermal expansion (CTE) was determined by Thermomechanical analysis (TMA) method using a Perkin Elmer TA7 instrument. The thermal stability of the composites was analyzed by thermogravimetric analysis (TGA) using TA Instruments model SDT 2960 thermal analyzer. The samples were heated from room temperature to 1000 °C at a heating rate of 100 °C/min in N_2 atmosphere. Specific heat of the composites was determined at different temperatures by DSC method in inert atmosphere at a heating rate of 10 °C/min according to ASTM D 3947-86. Hot wire method (ASTM C 1113) was used for

Table 2 Composition and density of the syntactic foams

Syntactic foams type	Weight percentage			Void (Vol%)	Density (kg/m^3)
	Phenolic resin	Microballoon	Fibre		
PS	55.6	44.4	–	5.0	570
PSF1	47.6	38.1	14.3	3.8	647
PSF2	43.5	34.8	21.7	3.9	688
PSF3	40.0	32.0	28.0	1.3	748
PSF4	37.1	29.6	33.3	1.2	798
PSF5	35.7	28.6	35.7	1.4	824
PSF1-M[a]	47.6	38.1	14.3	8.5	500

[a] Contains mixture of microballoons; K25 (density = 250 kg/m^3) and K37 (density = 370 kg/m^3) in equal weight ratio

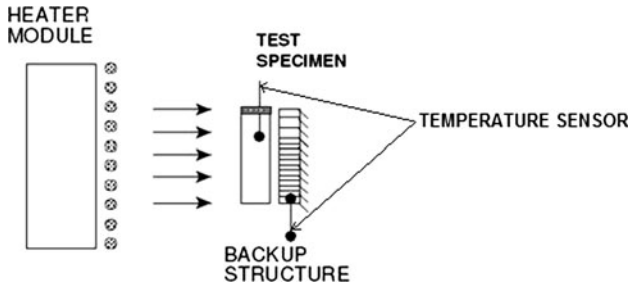

Fig. 1 Schematic of the aero-heating simulation facility

determining thermal conductivity [14]. The testing was done in Argon atmosphere at 1 atm pressure.

For aero-thermal tests, ablative composite block of dimension, 150 × 150 × 25 mm was bonded to CFRP-aluminium honey comb (11 mm thick) using a proprietary adhesive developed by VSSC. A black coating was given on the surface to enhance the emissivity of the surface to above 85%. Thermocouples were bonded to the interface and backwall of the ablative, and the surface was heated by IR lamp to simulate the heat flux. The schematic of the test setup is given in Fig. 1. The simulation of the required transient heat flux history is achieved by exposing the specimens to a time accurate radiation heating from an array of quartz enveloped tungsten filament IR lamps. The electrical power to the lamp is controlled in feedback mode, and the required instantaneous heat flux is simulated. Gardon-type heat flux sensors were used for heat flux measurements. The temperature sensors are positioned at a depth of 23 mm from the front wall (i.e. interphase between the substrate and composite) in the composite and at a total depth of 29 mm from the front wall. Heat flux was controlled (or regulated) using a thyristor-based power controller where the simulated heat flux was measured and used for correcting the power supplied to the heater modules in a closed loop feedback control. The specimens are instrumented for backwall temperature measurements using K-type thermocouples with a chain accuracy of ±1% of reading. The thermal data were logged using a PC-based data acquisition system.

Results and discussion

Silica-fibre reinforced phenolic syntactic foams with varying fibre loadings were processed. The photograph of a 15-mm thick ablative composite sample (PSF2) is shown in Fig. 2. In the case of PS, which contain no fibres, the microballoons are uniformly distributed (Fig. 3). It was observed that the unbundling of the chopped silica fibres was more effective at low fibre loadings. The SEM image of PSF1-M which is having the lowest fibre loading is shown in Fig. 4. The fibres are randomly distributed in the case of the composites with low fibre loadings. There is no preferential orientation in this case, and their distribution is

Fig. 2 Photograph of a 15-mm thick silica fibre-reinforced phenolic syntactic foam

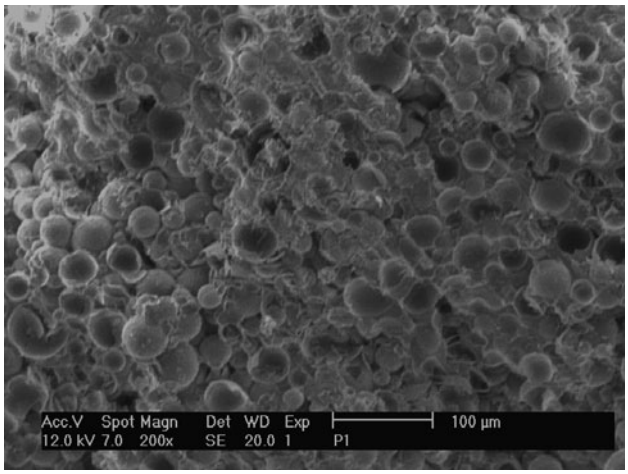

Fig. 3 SEM image of PS depicting uniform distribution of microballoons

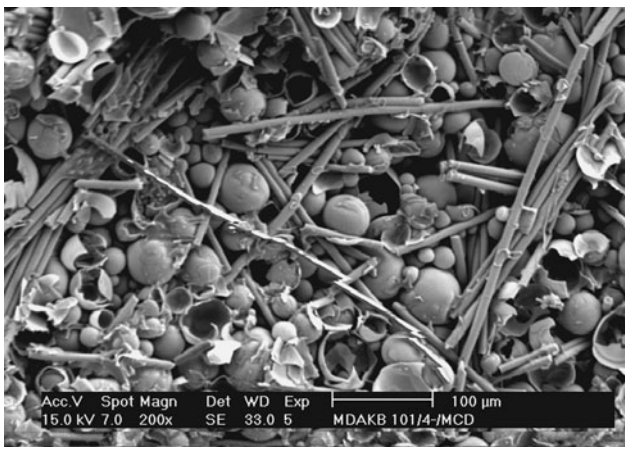

Fig. 4 SEM image of the foam composite (PSF1-M) with the lowest silica fibre concentration illustrating randomly distributed silica fibres

almost uniform in the matrix. Similar observations can be noted in the SEM image of PSF3 (Fig. 5). However, the SEM image of PSF5 (Fig. 6) which is having the highest fibre loading shows clustering of the fibres.

Mechanical properties

The mechanical properties of syntactic foams generally depend on density of the foam, which in turn depends on resin to filler ratio. In the case of fibre-reinforced syntactic foams, the concentration of fibre also plays an important role in determining the mechanical properties. The variation of mechanical properties of the syntactic foams with increase in volume percentage of silica fibre is shown in Fig. 7.

From Fig. 7, it is evident that tensile strength increased with fibre volume percentage in the composite and showed a maximum corresponding to 15 vol% of silica fibre (PSF4) and decreased on its further addition. When we compare the tensile strength of the fibre-reinforced syntactic foams with bare phenolic syntactic foams (PS), we can see that incorporation of fibre has little effect on tensile strength at low fibre loadings (PSF1 and PSF2). In the case of bare syntactic foams, a process involving resin fracture and resin–microballoon debonding, rather than crushing of the microballoons dominated the tensile failure as illustrated in the SEM image of PS (Fig. 3) [11, 15]. Apart from these failure modes, pull out of fibres also has to be considered in the case of fibre-reinforced syntactic foams. The decrease in tensile strength at higher loadings of silica fibre (after attaining a maximum value) has been ascribed to poor wetting of fibre and microballoon, due to decrease in resin content with increase in silica fibre loading. The poor wetting leads to easy debonding between filler and matrix at high volume fraction of fibre. Another factor which lowers the tensile strength is the clustering of fibres at high fibre concentrations. Due to clustering, the fibres are not effectively wet by the resin. As a result, the transfer of load from the matrix to the individual fibre is not effectively achieved. Figure 8a shows the clustering of fibres in the fracture surface of PSF5. Here, the failure occurred due to the debonding of fibre. Figure 8b shows the portion of the foam composite from where bunch of fibre has been removed during testing. The alignment of fibres in a direction perpendicular to the applied load also accounts for the decreased tensile strength for PSF5 (Fig. 8c). Similar observations of decrease in tensile strength after attaining a maximum value have been reported earlier [13].

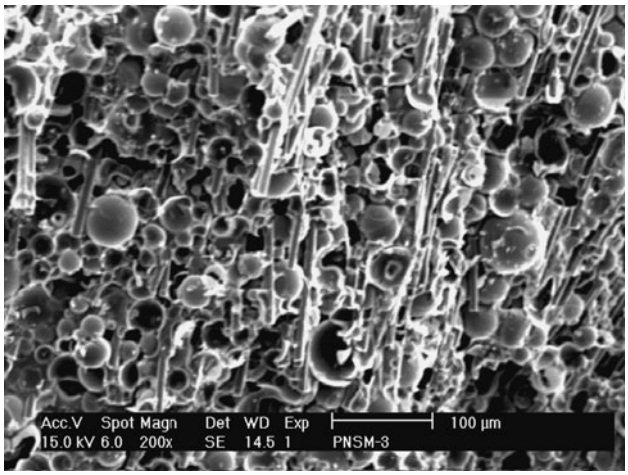

Fig. 5 SEM image of PSF3 showing unbundling of silica fibres

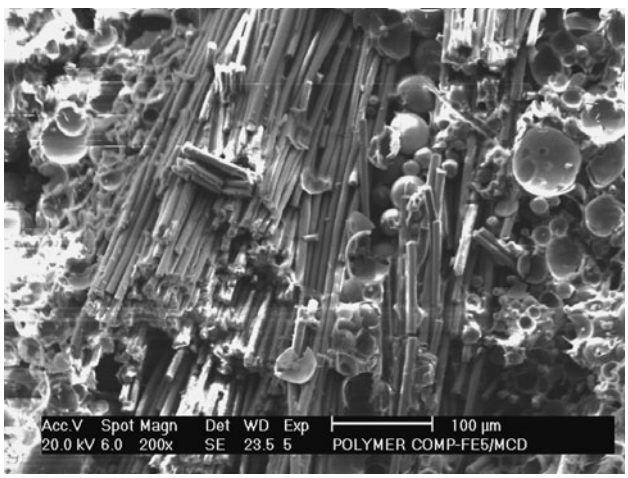

Fig. 6 SEM picture of PSF5 depicting bundling of silica fibres

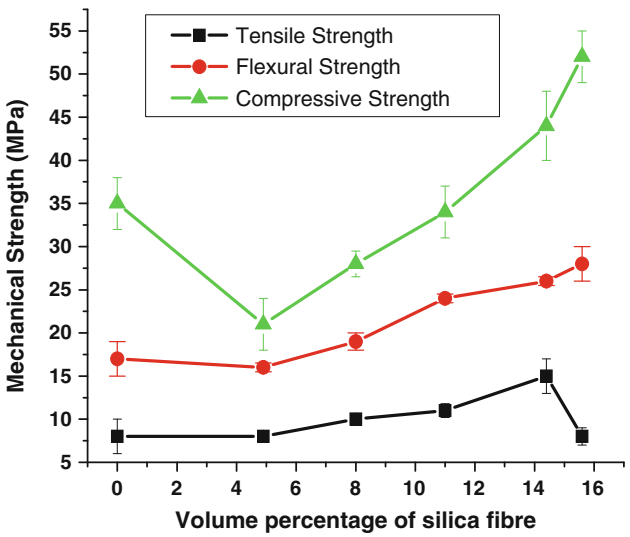

Fig. 7 Variation of mechanical properties with volume percentage of silica fibre

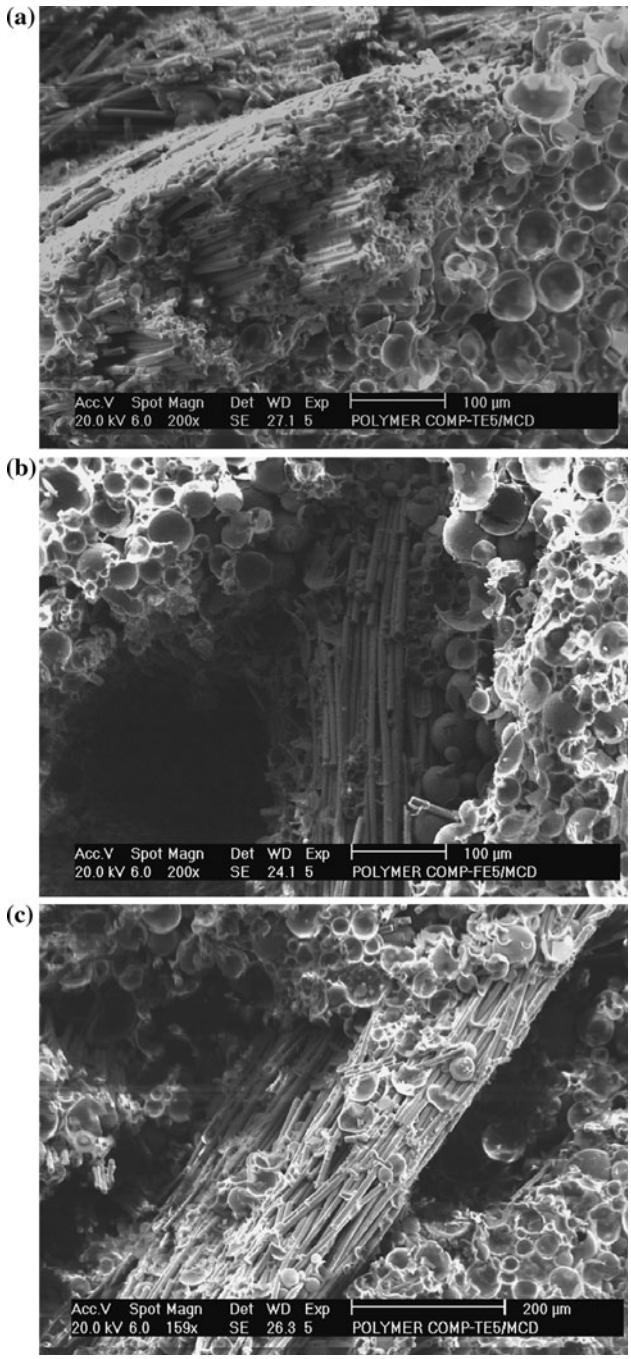

Fig. 8 SEM pictures of the foam composites showing fracture surface. **a** Depicts debonding of fibre-clusters in the case of PSF5. **b** Shows the area from where the fibre-cluster has been removed during flexural testing in the case of PSF5 and **c** shows the alignment of fibres in a direction perpendicular to the applied load (during tensile test) in PSF5

The flexural strength of the fibre-reinforced syntactic foams increased with increase in volume percentage of fibre. This general pattern of increase in strength values is ascribed to the better load-bearing capacity of the fibrous reinforcements, which are very effective in sustaining the load that is transferred on to them from the matrix. The cracks propagate in a straight manner for fibre-free syntactic foams; whereas some deviation is observed for fibre-reinforced syntactic foams, i.e. the fibres make the crack propagation path longer [13]. Both these features are shown in the photographs of the fractured specimen of PS and PSF5 (Fig. 9). It is reported that the failure process initiates first in the tensile side of the specimen and is followed by a sudden and catastrophic failure [16]. Also, it is known that when a material is subjected to flexural load, the upper part of the specimen experiences a compressive load normal to the plane and the lower part a tensile load parallel to the plane. For the sample PSF5, though the tensile strength is lower, the higher compressive component of the load makes the flexural strength higher.

The addition of small amounts of fibre resulted in lowering of compressive strength. However, at higher fibre loadings, the compressive strength showed higher values compared to bare phenolic syntactic foams. This increase in strength can be attributed to the load-bearing ability of the fibrous reinforcements. The compressive modulus values of the syntactic foams are given in Table 3. The modulus values also followed the same trend as the strength values. At low fibre concentration, the matrix is not restrained by enough fibres and therefore highly localized strains occur at a low stress, which causes the bond between the matrix and fibre to break leaving the matrix diluted by non-reinforcing debonded fibres. At high fibre loadings, the stress is more evenly distributed and hence the strength and the modulus values increase [17, 18].

The specific mechanical properties of the fibre reinforced syntactic foams are depicted in Fig. 10. The specific mechanical properties followed the same trend as the corresponding mechanical properties. The specific mechanical properties show that fibre reinforcement is an effective method for improving the mechanical properties of syntactic foams.

The tensile, flexural and compressive strength values for PSF1-M (7.5, 9.3 and 8 MPa, respectively) are lower compared to PSF1. This is attributed to the low strength of the K-25 microballoons. The specific flexural and compressive strength (0.0186 and 0.016 MPa/kg/m^3) are also lower than PSF1. However, specific tensile strength (0.015 MPa/kg/m^3) showed a higher value for PSF1-M. In general, the compressive strength and modulus of the ablative composites increased with both density and fibre content. The modulus of PSF1-M is much lower compared to PSF1, due to the low shell thickness (and low strength) of the K-25 microballoons and due to the high void content in PSF1-M.

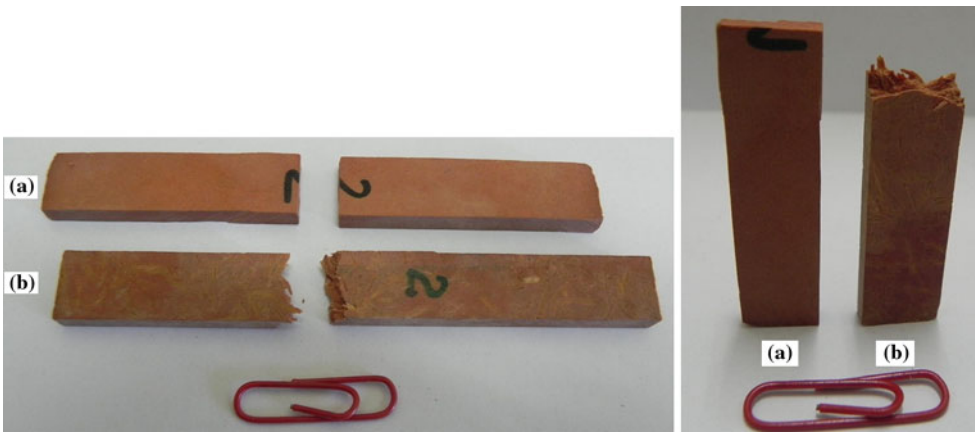

Fig. 9 Photographs of flexurally failed **a** PS and **b** PSF5 depicting fracture features

Table 3 Compressive modulus values of the syntactic foams

Sample code	Compressive modulus (MPa)
PS	1050
PSF1	940
PSF2	1020
PSF3	1190
PSF4	1390
PSF5	1670
PSF1-M	400

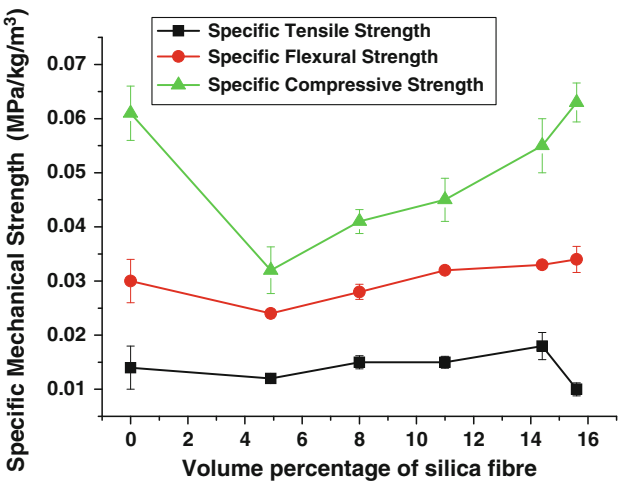

Fig. 10 Dependency of specific mechanical properties on fibre concentration

Dynamic mechanical analysis (DMA) of the syntactic foams

Dynamic mechanical analysis of the syntactic foams has been carried out to study the structural and viscoelastic behaviour. Many studies have been focussed on the dynamic mechanical behaviour of fibre-reinforced polymer composites, and some of the researchers have interpreted the properties of the fibre–matrix interface of the composites using DMA data [19]. The dynamic mechanical properties of syntactic foams have been reported in literature [2, 20]. The variation of storage modulus and tan delta with temperature (from 30–300 °C) has been studied for bare phenolic syntactic foam and fibre-reinforced phenolic syntactic foams.

Storage modulus

The variation of storage modulus of the syntactic foams with temperature is depicted in Fig. 11. It is found that the storage modulus values of the syntactic foams showed a gradual decrease initially (due to increased segmental mobility) followed by a steep decrease around the glass transition region. In the rubbery region, there is not much change in storage modulus of the syntactic foams. In the glassy region, the components are in a frozen state. In such a state, there exists a close and tight packing in the composite resulting in high modulus. As temperature increases, the components in the composite become more mobile and lose their close packing arrangement. Thus, the decrease in storage modulus with temperature is due to the increased viscoelastic deformation of the matrix. The storage modulus values of fibre reinforced syntactic foams are remarkably higher than that of bare syntactic foams in the temperature range used in this study, i.e. reinforcement enables efficient stress transfer from matrix to fibre. This also indicates that the incorporation of fibre in syntactic foam induces reinforcing effects appreciably at higher temperatures also. This shows the importance of fibre reinforcement in syntactic foams. There is no particular trend in the variation of the dynamic mechanical properties with silica fibre concentration. The difference between the storage modulus of the composites in the glassy and rubbery region is higher for fibre-reinforced systems compared to the bare syntactic foam. Thus, the effect of fibre reinforcement is more pronounced in the glassy region.

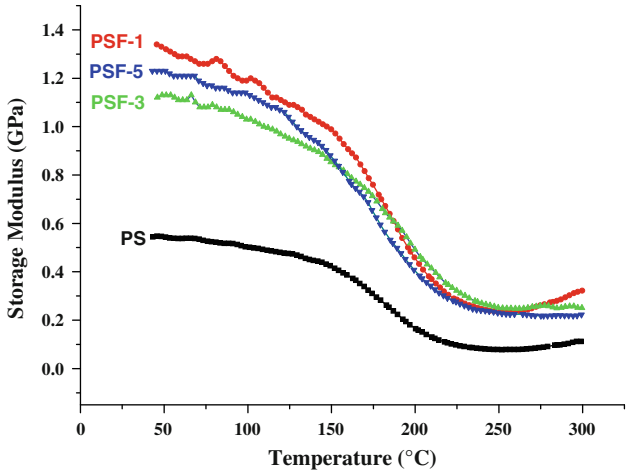

Fig. 11 Variation of storage modulus of the syntactic foams with temperature

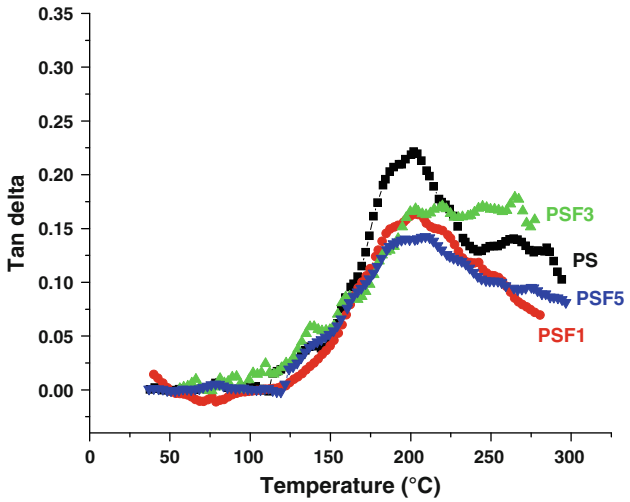

Fig. 12 Effect of temperature on tan delta of the syntactic foams

Tan delta

The low-density ablative TPSs when used in launch vehicles are subjected to severe vibration during the launching manoeuver. Hence their damping characteristics are significant. The variation of damping factor, tan delta which is the ratio of loss modulus to storage modulus (E''/E'), as a function of temperature is shown in Fig. 12.

The tan delta height is found to be higher for plain phenolic syntactic foams compared to fibre-reinforced ones. The difference in tan delta values of the fibre-free and fibre-reinforced syntactic foams is prominent at the regions of tan-delta maximum. Tan delta reflects the mobility and movement capacity of molecular chain segments during glass transition. Tan delta is also a measure of the ratio of energy dissipated as heat to the maximum energy stored in the material. Therefore, more energy is stored in the material at low values of tan delta. Lower tan delta height of the fibre-reinforced system shows good interfacial adhesion between the fibre and the matrix; therefore, the movement of polymer molecules is restricted. The incorporation of fibres acts as barrier to the mobility of polymer chains leading to low flexibility and low degrees of molecular motion and hence low damping characteristics. Also, the lowering of tan delta is due to the fact that there are fewer matrices by volume to dissipate the vibrational energy. The T_g values of the syntactic foams are not much affected by fibre reinforcement.

CTE

Coefficient of thermal expansion is an important design parameter for the materials intended to be used for structural applications. The mismatch in the expansion coefficient of different materials in a system can lead to thermal strain in the material, leading to its failure in spite of having the required strength. Therefore, it is required to have a knowledge of the CTE of the ablative composites to be used in TPSs. In the present system, since the microspheres, silica fibres and air voids are distributed randomly throughout the polymer matrix, the thermophysical properties are independent of the orientation of the foam. The linear expansion of the ablative composites was studied as a function of temperature from 30 to 200 °C at a heating rate of 10 °C/min. The curve showed two different slopes for all the compositions (one in the range, 30–125 °C and other in the range, 125–200 °C). The variation of linear thermal expansion of the ablative composites with increase in temperature is shown in Fig. 13. The inflection point at around 150 °C is due to the glass transition. CTE of the ablative composites has been calculated for these two temperature ranges, and the results are tabulated in Table 4.

From Table 4, it is found that the CTE of the ablative composites are in the range varying from 15 to 26 $\times$ 10^{-5}/°C for the temperature range 30–125 °C and from 33 to 51 $\times$ 10^{-5}/°C for the range 125–200 °C. The higher linear expansion coefficients in the temperature range 125–200 °C are expected due to the higher expansion of the phenolic resin above its glass transition temperature. The low value of CTE for PSF1-M is ascribed to its higher void content.

TGA

Thermogravimetric analysis was used to investigate the thermal decomposition characteristic of the ablative composites. TGA of the ablative composites was carried out over a wide range of temperatures from ambient to 1000 °C. Figures 14 and 15 show TGA curves and DTG

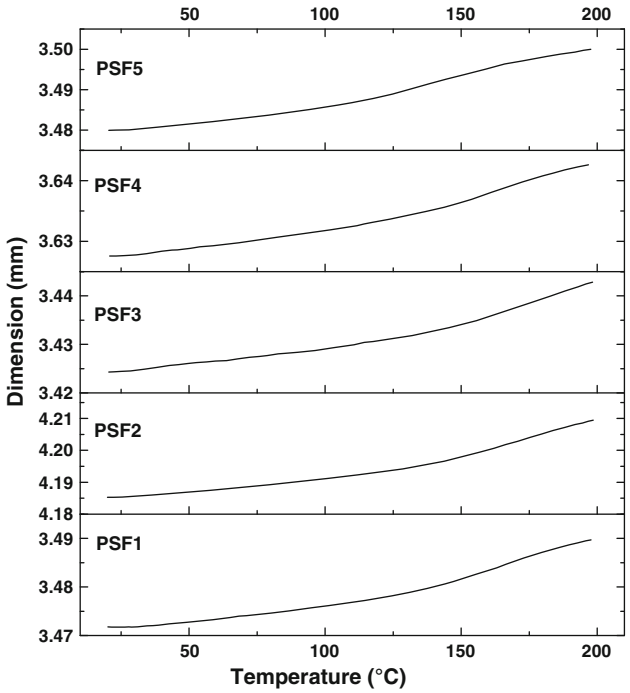

Fig. 13 Variation of linear expansion with temperature for the ablative composites

Table 4 CTE values of the ablative composites

Syntactic foam code	Coefficient of thermal expansion, α (10^{-5}/°C)	
	30–125 °C	125–200 °C
PSF1	19	45
PSF2	21	51
PSF3	20	46
PSF4	16	34
PSF5	26	43
PSF1-M	15	33

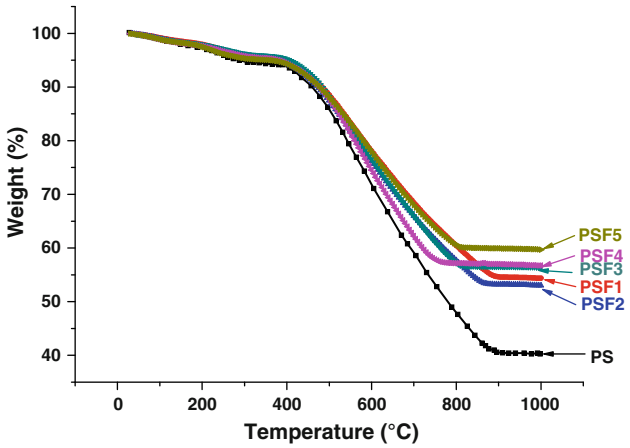

Fig. 14 Thermal decomposition patterns of the ablative composites

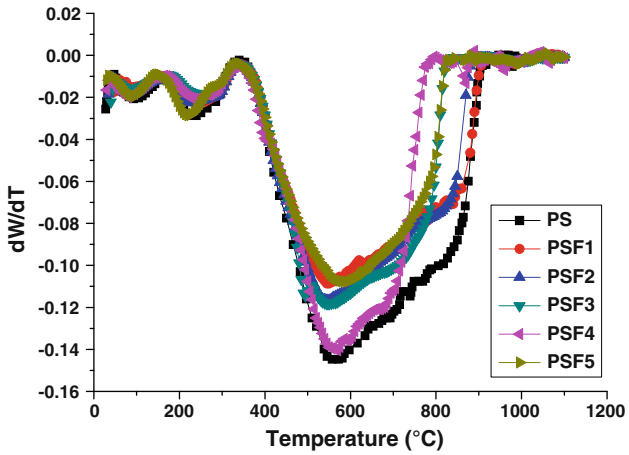

Fig. 15 DTG curves of the ablative composites

Table 5 Specific heat of the virgin material at different temperatures

	Specific heat of virgin material (cal/g/°C) (N_2 atmosphere)			
	80 °C	100 °C	120 °C	140 °C
PSF2	0.35	0.35	0.36	0.36
PSF4	0.31	0.31	0.31	0.32
PSF1-M	0.34	0.36	0.37	0.38

curves of the ablative composites in the temperature range from ambient to 1000 °C at a heating rate of 100 °C/min in N_2 atmosphere. It can be seen from the figure that the composites showed no mass loss after 800 °C. The char residue for PSF2 is less than that of PSF1, even though PSF2 has higher fibre loading. PSF3 and PSF4 exhibited almost the same char residue. All these imply the presence of macro zones more rich in fillers in the composite and the possibility for the presence of unbundled silica fibres. It can also be seen that fibre-reinforced foam composites exhibited improved thermal stability compared to the unreinforced ones.

Specific heat of syntactic foams

Specific heat is a significant property of ablative composites. The specific heat values for the ablative composites (both virgin and pyrolysed) at different temperatures are given in Tables 5 and 6, respectively. The specific heat values measured for phenolic resin, K-37 microballoon and silica fibre at 80 °C are 0.418, 0.179 and 0.296 cal/g/ °C, respectively. The specific heat values are low for systems with high fibre concentration due to the low specific heat of the fibre, compared to the resin. The specific heat values showed a marginal increase in value with increase in temperature from 80 to 140 °C for all the compositions. The specific heat values of pyrolysed samples are lower than that of the virgin material due to low specific heat of the carbonized matter (Table 6).

Table 6 Specific heat of the pyrolysed material at different temperatures

	Specific heat of pyrolysed material (cal/g/°C) (N_2 atmosphere)			
	80 °C	150 °C	200 °C	250 °C
PSF2	0.25	0.27	0.29	0.30
PSF4	0.29	0.30	0.32	0.32
PSF1-M	0.22	0.23	0.23	0.24

Thermal conductivity

The thermal conductivity of ablatives plays an important role in determining the temperatures of components and payloads during the on-orbit and re-entry phases of the mission. The effective thermal conductivity of a composite depends upon the conductivity of the individual components and the interconnectivity of the higher conducting phase [21, 22]. Thermal conductivity of the ablative composites increased with fibre concentration (and hence density) and temperature. Thus, amongst the three compositions (PSF2, PSF4 and PSF1-M), PSF4 containing 33% of silica fibre exhibited the highest thermal conductivity at all temperatures. The low conductivity in the case of PSF1-M is due to the lack of better interconnectivity amongst the components in it. The variation of thermal conductivity with temperature is shown in Fig. 16. For foam materials, thermal conductivity and temperature are related by the equation

$$K_{\text{eff}} = K_{\text{o}} + \beta\,(T - 273.15)$$

where K_{eff} is the effective thermal conductivity at temperature, T (in Kelvin), K_{o} is thermal conductivity at $T = 273.15$ K and β is the temperature coefficient of thermal conductivity. The values of K_{o} and β were obtained from the slope and y intercept of the thermal conductivity versus temperature plot, respectively. The values of K_{o} and β for the foam composites are given in Table 7. The value of β increased with increase in density of the composites. The value of β is the lowest for PSF1-M due to its minimum mechanical compaction.

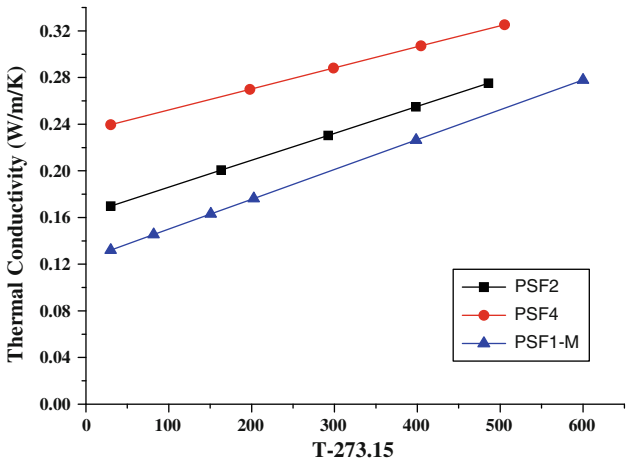

Fig. 16 Thermal conductivity of the foam composites as a function of temperature

Thermal response evaluation studies

Thermal response evaluation studies were carried out to evaluate the TPS performance at regions exposed to moderate re-entry heating conditions. Heating pattern is basically expected to vary from location to location on the vehicle as a scaled variant of one another, with the exception of the point of boundary layer transition. In order to generalize the environments and also to compare the TPS performance between regions experiencing moderate re-entry heating, normalized heat flux (obtained from Eckert's reference enthalpy method) was considered. Normalization was undertaken with respect to the stagnation region in this study.

Aero-heat flux incident on a 25° cone following a ballistic re-entry trajectory is shown in Fig. 17. Aerodynamic heating increases monotonically with decreasing altitude during re-entry (considered at time, $t = 0$ s at 120 km altitude), where the density of air also increases monotonically till the peak heating. Subsequently, even with increasing density with re-entry, due to the reducing velocity, the aerodynamic heating decreases till it touches down. This pattern is typical of all earth re-entry vehicles.

Two compositions (PSF1-M and PSF2) were evaluated by the thermal simulation tests to select the optimum system and to study the influence of higher silica fibre content

Table 7 The values of K_{o} and β for the foam composites

Sample reference	K_{o} (W/mK)	β (10^{-4} W/mK^2)
PSF2	0.163	2.3
PSF4	0.234	1.8
PSF1-M	0.124	2.6

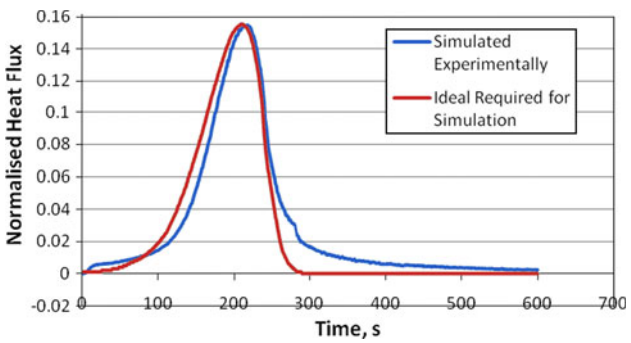

Fig. 17 Aero-heat flux on a 25° cone on ballistic re-entry

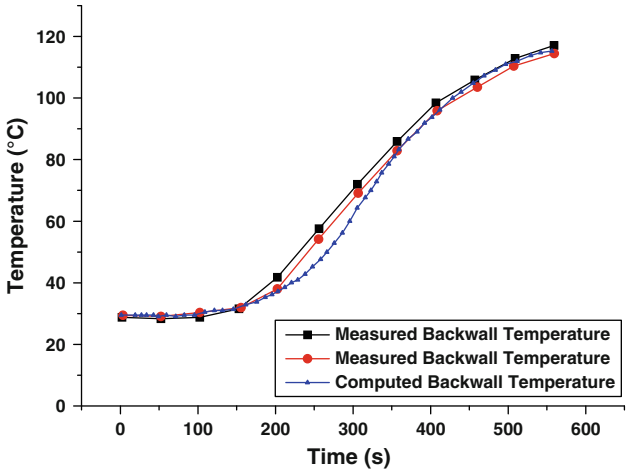

Fig. 18 Theoretical prediction of backwall thermal response and the experimental behaviour (at two locations) of 25-mm thick ablative TPS, PSF1-M

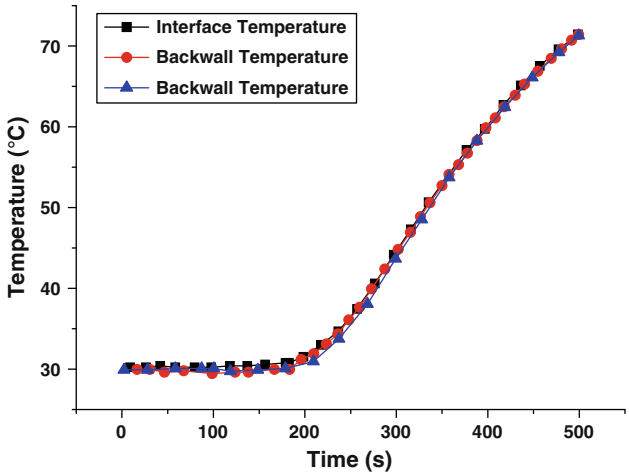

Fig. 19 Thermal response of 25-mm thick ablative TPS-PSF2 performance during experiment

on the TPS performance during re-entry. The composition of the composites is given in Table 2. Structural integrity of the test specimen and its physical performance like gas evolution, fire on the TPS etc. were examined.

Gas evolution and fire were observed during the test due to combustion of the evolved products. Surface of the test specimen exhibited micro cracks after the test. However, total delamination did not occur. During the tests, moderate ablation occurred in both the cases, and the char thickness to the extent of about 2–5 mm was measured using a vernier. The backwall thermal response for PSF1M with the design thickness of 25 mm is shown in Fig. 18. For the 25° cone region, the incident heat flux is very high, about 15% of the stagnation heating. At 500 s (the expected flight duration), the backwall temperature is 110 °C which is less than the temperature constraint (150 °C). The total weight loss of the specimen is around 7.7%. The theoretical time–temperature graph was computed considering the material properties (thermal conductivity, density, heat capacity, heat of decomposition, rate of decomposition etc.) for both virgin material and the char under the simulated heat flux conditions as, for example, Fig. 17.

The thermal response of the ablative with enhancement in silica fibre content resulted in TPS with low backwall temperatures (71 °C at 500 s) and also superior mechanical properties but has a higher density (680 kg/m^3). Thermal response of PSF2 is given in Fig. 19. PSF2 exhibited reduced charring and mass loss compared to PSF1-M.

Figure 20a and b shows the photograph of PSF1-M before and after the aero-heat simulation test, respectively. Figure 21 shows the SEM picture of PSF1-M after aero-heat simulation test. SEM picture of the samples after the test shows coalescence and shrinkage of microballoons. However, the charred surface remained intact after the test.

Since the aero-shear loads are very low for ballistic re-entry trajectories, for the moderate heat flux condition, PSF1-M with low density (and hence mass advantage) is better suited for thermal protection as it satisfies the requirements of structural integrity and temperature constraints.

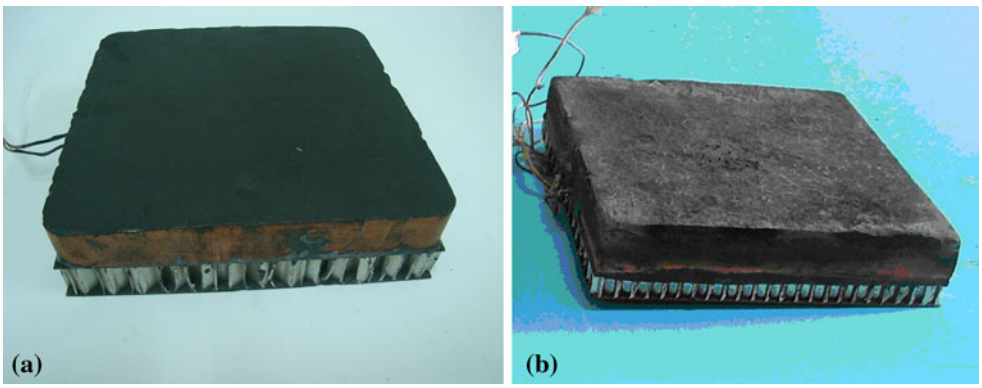

Fig. 20 Photograph of PSF1-M **a** before and **b** after aero-thermal test (The *black colour* on the surface of the sample in **a** is emissivity coating)

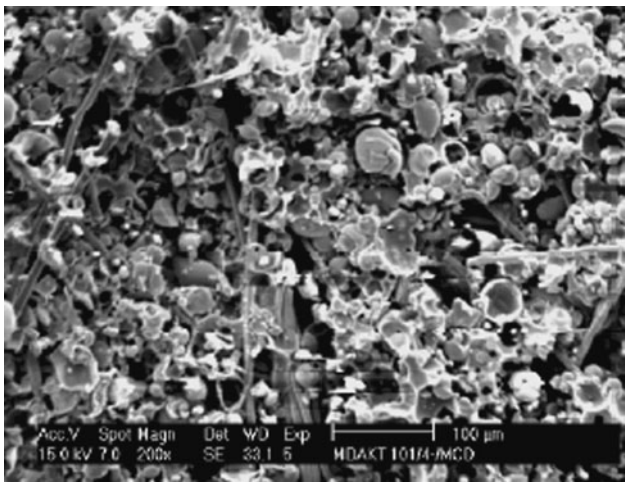

Fig. 21 Charred surface of PSF1-M after aero-thermal tests

Conclusions

Silica fibre-reinforced phenolic syntactic foams containing varying concentration of the fibre and different specific gravities were realized. Tensile strength and specific tensile strength increased with fibre concentration and attained the maximum at 15% by volume of silica fibre and decreased thereafter due to poor wetting of the fibre as evidenced by SEM analysis. Flexural and compressive strength increased with increase in fibre concentration. The storage modulus showed higher values for the fibre reinforced systems whereas tan delta values were reduced by fibre reinforcement. CTE of the composites varied from 15 to 26 $\times$ 10^{-5}/°C in the temperature range 30–125 °C and from 33 to 51 $\times$ 10^{-5}/°C in the range 125–200 °C. TGA studies show that char residue increased with inorganic content and there is no mass loss for the composites beyond 800 °C. Specific heat decreased with increasing fibre concentration for the virgin material and for the pyrolysed composites, and the values were low for composites with high resin concentration. Thermal response of the ablatives was measured by simulating a moderate atmospheric re-entry heat flux history on the specimen with maximum heat flux of about 15% of stagnation heating for a duration of 600 s. Simulations showed that, for given syntactic foam, silica fibre reinforcement is conducive for reducing the backwall temperature and enhancing the mechanical properties. Results generated from the test serves as benchmark data for the thermal response of medium-density ablative TPS materials and offset the uncertainty in thermophysical data at elevated temperatures. The robustness of the medium-density ablative was brought out, proving it as a viable alternative for immediate application in a single-use re-entry mission. This design option can result in significant reduction in developmental costs and lead time to undertake a re-entry mission.

Considering the mass advantage and acceptable mechanical, thermal and thermomechanical properties, the medium-density ablative PSF1-M with a specific gravity of 0.5 is suited for thermal protection of earth re-entry systems.

Acknowledgements The authors acknowledge Director, VSSC for granting permission to publish this article. Dr. K. Ambika Devi and Dr. Korah Bina Catherine (ASD) are acknowledged for mechanical testing and thermal analysis, respectively. Shri. S. Krishnamoorthy (PRG) is acknowledged for the thermal conductivity measurements and Shri. Ramesh Narayanan (MCD) for SEM analysis. Credit is also due to Shri TV Radhakrishnan, Shri Sundar B, Shri S Jeyarajan and Smt K Vanitha of AHTD for design and test support during the aero-thermal studies.

References

1. Bahramian AR, Kokabi M, Famili MHN, Beheshty MH (2006) Polymer 47:3661
2. John B, Nair CPR, Ninan KN (2007) Cell Polym 26:229
3. John B, Nair CPR (2010) Update on syntactic foams. iSmithers Rapra, UK
4. Okuno K, Woodhams RT (1974) J Cell Plast 10:237
5. Sunshine N (1973) In: Kuryla W, Papa J (eds) Flame retardancy of phenolic materials. Marcel Dekker, New York
6. Sreejith PS, Krishnamurthy R, Malhotra SK, Narayanasamy K (2000) J Mater Process Technol 104:53
7. Re-entry Technology: Atmospheric Re-entry Demonstrator, European Space Agency, Directorate of Manned Spaceflight and Microgravity. http://www.estec.esa.nl/spaceflight/index.htm
8. Guthrie JD, Battat B, Severin BK. Advanced materials and process technology. Defense Technical Information Centre, IIT Research Institute, New York. http://www.amptiac.iitri.org
9. Torre L, Kenny JM, Boghetich G, Maffezzoli A (2000) J Mater Sci 35:4563. doi:10.1023/A:1004828923152
10. Gupta N, Karthikeyan CS, Sankaran S, Kishore (1999) Mater Charact 43:271
11. Karthikeyan CS, Sankaran S, Kishore (2005) Macromol Mater Eng 290:60
12. Karthikeyan CS, Sankaran S, Kishore (2004) Mater Lett 58:995
13. John B, Nair CPR, Ninan KN (2008) Polym Polym Compos 16:431
14. Kumar SK, Krishnamoorthy S, Rao SVS (2006) In: 9th AIAA/ASME joint thermophysics and heat transfer conference, San Francisco, California, 5–8 June 2006
15. John B, Nair CPR, Devi KA, Ninan KN (2007) J Mater Sci 42:5398. doi:10.1007/s10853-006-0778-0
16. Karthikeyan CS, Sankaran S, Kishore (2000) Polym Int 49:158
17. Joseph PV, Mathew G, Joseph K, Groeninckx G, Thomas S (2003) Compos A Appl Sci Manuf 34:275
18. Joseph PV, Joseph K, Thomas S (1999) Compos Sci Technol 59:1625
19. Yu XB, Wei C, Zhang FA (2006) Polym Adv Technol 17:534
20. Sankaran S, Sekhar KR, Raju G, Kumar MNJ (2006) J Mater Sci 41:4041. doi:10.1007/s10853-006-7607-3
21. Agarwal R, Saxena NS, Sharma KB, Thomas S, Pothan LA (2003) Indian J Pure Appl Phys 41:448
22. Idicula M, Boudenne A, Umadevi L, Ibos L, Candau Y, Thomas S (2006) Compos Sci Technol 66:2719